
Article:
Schlund, M., Scipal, K. and Quegan, S. orcid.org/0000-0003-4452-4829 (2018) Assessment of a power law relationship between P-band SAR backscatter and aboveground biomass and its implications for BIOMASS mission performance. IEEE Journal of Selected Topics in Applied Earth Observations and Remote Sensing, 11 (10). pp. 3538-3547. ISSN 1939-1404

https://doi.org/10.1109/jstars.2018.2866868

Assessment of a Power Law Relationship Between P-band SAR Backscatter and Aboveground Biomass and its Implications for BIOMASS Mission Performance

Michael Schlund, Klaus Scipal, and Shaun Quegan

***Abstract*—This paper presents an analysis of a logarithmic relationship between P-band cross-polarized backscatter from Synthetic Aperture Radar (SAR) and aboveground biomass (AGB) across different forest types based on multiple airborne data sets. It is found that the logarithmic function provides a statistically significant fit to the observed relationship between HV backscatter and AGB. While the coefficient of determination varies between datasets, the slopes and intercepts of many of the models are not significantly different, especially when similar AGB ranges are assessed. Pooled boreal and pooled tropical data have slopes that are not significantly different, but they have different intercepts. Using the power law formulation of the logarithmic relation allows estimation of both the Equivalent Number of Looks (ENL) needed to retrieve AGB with a given uncertainty and the sensitivity of the AGB inversion. The campaign data indicates that boreal forests require a larger ENL than tropical forests to achieve a specified relative accuracy. The ENL can be increased by multi-channel filtering, but ascending and descending images will need to be combined to meet the performance requirements of the BIOMASS mission. The analysis also indicates that the relative change in AGB associated with a given backscatter change depends only on the magnitude of the change and the exponent of the power law, and further implies that to achieve a relative AGB accuracy of 20% or better, residual errors from radiometric distortions produced by the system and environmental effects must not exceed 0.43 dB in tropical and 0.39 dB in boreal forests.**

***Index Terms*—P-band synthetic aperture radar (SAR), aboveground biomass retrieval, forestry, BIOMASS mission.**

I. Introduction

FORESTS play a key role in the global carbon cycle and climate change, acting as sinks for CO_2 when growing and sources of CO_2 when disturbed [1]. Information on forest biomass, its spatial distribution and change over time is therefore essential in estimating the global carbon balance [2]; this has led to major efforts to estimate aboveground forest biomass (AGB) from satellite data using passive microwave [3] and LiDAR sensors [4], [5], and combinations of different sensors [5]–[7]. Another key technology for this purpose is Synthetic Aperture Radar (SAR) operating at L- or P-band (wavelengths around 24 and 70 cm respectively), which yield much higher sensitivity to AGB than shorter wavelengths [8]–[10]. This is the rationale underlying the European Space Agency (ESA) BIOMASS mission, ESA's 7th Earth Explorer [11], which will carry a fully polarimetric P-band SAR capable of providing near-global, spatially explicit measurements of forest height, biomass and biomass change.

The use of P-band SAR builds on a long research heritage which suggests a logarithmic relationship between AGB and the cross-polarized backscatter γ^0_{HV} (where HV indicates horizontal-vertical polarization). The backscattering coefficient γ^0_{HV} is defined as $\gamma^0_{HV} = \sigma^0_{HV}/\cos\theta$, where σ^0_{HV} is the normalized radar cross section and θ is the local incidence angle. This relationship was reported for data collected in forests in northern boreal and hemi-boreal latitudes [10], [12]–[15], the temperate zone [8]–[10] and the tropics [9], [10], [16]–[19]. A similar relationship was also found for other wavelengths in various biomes [9], [13], [16], [18], [20]. All these studies evaluated the logarithmic relationship at only one or a few sites and mostly in a single biome. As a result, the empirical basis for this model has not been rigorously assessed and its validity and generality has been questioned [21]. For example, poor correlation and high uncertainty were reported when parameters of the regression model found in a boreal site were transferred to a hemi-boreal site and vice versa [15].

Based on a thorough and consistent analysis using available campaign data from boreal, hemi-boreal, temperate and tropical forests, as well as a temperate forest plantation, it is shown that for all sites considered there is a statistically significant logarithmic relationship between γ^0_{HV} and AGB. In addition, a covariance analysis (ANCOVA) is performed to evaluate the consistency of the model parameters between sites (Section IV). Having established the generality of the logarithmic backscatter-AGB relationship, we use its equivalent power law form to quantify how backscatter measurement uncertainty due to speckle affects AGB retrieval accuracy and also the implications for estimating biomass change (Section V).

It should be noted that some authors have used combinations of the polarimetric channels in estimating AGB [15], [19], essentially to minimize the effects of soil moisture or topography on the HV signal before developing the logarithmic relationship between HV backscatter and AGB. A more complex

M. Schlund is with the University of Goettingen, Goldschmidtstr. 5, 37077 Goettingen, Germany (e-mail: michael.schlund@uni-goettingen.de).

K. Scipal is with the European Space Agency, 2200 AG Nordwijk, The Netherlands (e-mail: klaus.scipal@esa.int).

S. Quegan is with the School of Mathematics and Statistics, University of Sheffield, Sheffield, U.K , and the U.K National Centre for Earth Observation (e-mail: s.quegan@sheffield.ac.uk).

Manuscript received xxxx; revised xxxx. This work was supported by Postdoctoral Research Fellowship Program of ESA and ESA's BIOMASS mission project.

model involving the intensity of the HH, VV and HV channels has also been used to estimate biomass [22]. Nevertheless, the logarithmic model gives a first order approximation that is adequate for estimating the equivalent number of looks (ENL) needed for BIOMASS to meet a given AGB accuracy. This is shown to have strong implications for data processing. In addition, a related analysis can be used to quantify the sensitivity to system errors.

II. Data

We analyze data from airborne P-band campaigns in the boreal, hemi-boreal, temperate and tropical forest biomes (Tab. I), gathered from forests in La Selva, Costa Rica [18], Mabounie and Lopé, Gabon [23], Paracou, French Guiana [24], Alaska and Maine, USA [12], [13], Remningstorp and Krycklan, Sweden [25], [26], and Landes, France (which is the single example of a plantation forest in the dataset) [8]. The NASA-JPL AirSAR system acquired P-band SAR data over La Selva, Alaska, Maine and Landes, while the DLR E-SAR system was used over Remningstorp and Krycklan, the DLR F-SAR system over Mabounie and Lopé and the ONERA SETHI system over Paracou. For Remningstorp, multi-temporal acquisitions were performed to capture the substantial differences in soil moisture occurring at this site and their impact on the signal [14]. Acquisitions with different flight headings were used in Remningstorp, Krycklan and Lopé in order to evaluate the sensitivity of the model to topography. The backscatter coefficients γ^0_{HV} at HV polarization were calculated consistently for all datasets in order to achieve a first order topographic correction.

Spatially and temporally collocated forest plots or stand data with AGB measurements were available for each study site. Diameter at breast height and tree height were measured in the field within plots, and species- or biome-specific allometries were then used to estimate AGB for individual trees, from which the AGB for each plot was computed [8], [12], [13], [18], [23]–[26]. Based on plot data, stand level AGB was further estimated for the boreal/temperate and plantation sites [8], [12], [13], [25], [26]. One exceptional case was Remningstorp, where additional laser scanning data, together with plot- and species-stratified information, supported the estimation of AGB for the stands [15]. Descriptions of the in situ datasets are provided in the references in Table I. In general, we assumed that the available AGB information is accurate at stand or plot level and thus sufficient for the purpose of this study.

TABLE I
Study Sites and average AGB (with AGB range in brackets) of collocated forest plots. N is the Number of Collocated Forest Plots Used in This Study.

Biome	Site	AGB (t/ha)	N	Reference
Tropical	La Selva	138 (7-270)	28	[18]
	Mabounie	309 (175-465)	7	[23]
	Lopé	264 (60-370)	8	[23]
	Paracou	393 (330-474)	24	[24]
Boreal & temperate	Alaska	108 (1-231)	20	[12]
	Maine	131 (0-331)	37	[13]
	Remningstorp	138 (11-287)	58	[25]
	Krycklan	99 (27-183)	27	[26]
	Landes	90 (0-153)	22	[8]

III. Logarithmic and power law relationships between aboveground biomass and HV backscatter

In this section we consider two equivalent representations of the relationship between AGB and HV backscatter. The first is a logarithmic relationship:

$$\gamma^0_{HV}[dB] = a \log_{10} \text{AGB} + b \tag{1}$$

where a and b are model parameters. We will use this form to estimate the fitting parameters a and b and test whether this relationship is statistically significant. Equation (1) can be regrouped as a power law:

$$\text{AGB} = 10^{-b/a} (\gamma^0_{HV})^p \tag{2}$$

where γ^0_{HV} is in natural units and $p = \frac{10}{a}$. This form is better for analyzing the consequences of this relation for BIOMASS performance.

A. Evaluation of the logarithmic relationship between AGB and HV backscatter

Linear least squares regressions were performed on the logarithmic form of the relation between HV backscatter and AGB (1). In the fitting process, only forest plots or stands with an AGB greater than 10 t/ha were considered, in order to exclude non-forest stands/plots. We also generated various diagnostics to test the appropriateness of a linear fit, by namely plots of the residuals against fitted values, quantile-quantile plots, scale-location plots, and residuals versus leverage plots (Cook's distance plots) [27], [28]. The coefficient of determination was also calculated to estimate the fraction of variance explained by the model [29], [30]

$$R^2 = 1 - \frac{SS_{Res}}{SS_{Tot}} \tag{3}$$

where SS_{Res} is the residual sum of squares and SS_{Tot} the total sum of squares. The F-test and corresponding p-values in the linear models were used to estimate the overall significance of the linear regression. Model coefficients were calculated for each individual site and for the pooled tropical and boreal sites.

B. Comparison of the log-log relationship between sites

The estimated slope a and intercept b in (1) vary from site to site. We performed an Analysis of Covariance (ANCOVA) to analyse the dependence of these coefficients between sites. ANCOVA is typically used to compare two or more regressions by testing the effect of a categorical factor (in our case the site) on a dependent variable (γ^0) while controlling for the effect of a continuous co-variable (AGB) [27], [28]. In practice, a dummy variable coded as 0 or 1 was introduced in order to add the categorical factor (Site) to the linear models [28]. Two models for the pairwise combination of sites were tested:

- Model 1: Separate regressions with different slopes for each site.
- Model 2: Separate regressions with the same slopes but different intercepts for each site.

Model 1 included, in addition to AGB and Site, an interaction term between AGB and Site, and the F-statistic and p-value were calculated to estimate the significance of the different terms. Model 1 thus has the form

$$\gamma^0 = b + a\log_{10}\text{AGB} + c\text{Site} + d\log_{10}(\text{AGB})\text{Site} \quad (4)$$

where here and in what follows we have dropped the HV subscript on γ^0. Confidence levels for the significance are based on p-values of 90%, 95%, 99% and 99.9%. A significant interaction term indicates that the slope was different between the sites, otherwise there is no evidence that the two fitted lines are not parallel [27], [28].

The difference of the intercept terms was further analyzed only for those combinations whose slopes were not significantly different (i.e. testing Model 2), since there is no provision within ANCOVA for comparing intercepts for models with significant different slopes [27]. The interaction term was removed, resulting in a regression model of the form:

$$\gamma^0 = b + a\log_{10}\text{AGB} + c\text{Site} \quad (5)$$

The categorical variable Site was again coded as 0 for one site and 1 for the other. Therefore, the models could be rearranged as

$$\gamma^0_{Site1} = b + a\log_{10}\text{AGB} \quad (6)$$

$$\gamma^0_{Site2} = b + a\log_{10}\text{AGB} + c \quad (7)$$

$$= (b + c) + a\log_{10}\text{AGB}. \quad (8)$$

A small value of c suggests little difference in intercept between the two sites. A significant effect of the site on the dependent variable (i.e., p-value inside the confidence interval) implies a significant difference of the intercept between the sites, in which case the linear fits are parallel but distinct. If the slopes and intercepts of the two fits do not differ significantly, there is no evidence that they are not identical.

IV. Results

Plots of γ^0_{HV} against $\log_{10}$ AGB for the pooled boreal/temperate and pooled tropical forest data, together with the associated diagnostics, are presented on the left and right sides of Fig. 1 respectively. Visual analysis of the plots strongly suggests a linear relationship in log-log space between AGB and HV backscatter. Both the plots of the residuals against the fitted values and the scale-location plots show no systematic deviation from a horizontal line, which would indicate that the linear model is not a good fit to the data. The residuals are normally distributed since they follow a straight line in the quantile-quantile plot. This conclusion is also supported by the p-values of the F-test statistics at the individual sites, which show that the relationship between γ^0_{HV} and $\log_{10}$ AGB is significant at the 99.9% level for all sites except Mabounie and Krycklan h_2 (significance of 99%) and Lopé and Krycklan h_1 (significance of 95%) (Tab. II).

TABLE II
Overview of P-band HV Backscatter and AGB Relationships for Various Study Sites. h_i Indicates Different Flight Headings. Tropical and Boreal indicate Statistics Derived by Combining All Respective Data Into One Sample.

	Site	a	b	$p = \frac{10}{a}$	R^2	p-value
Tropical	La Selva	6.09±0.34	-28.1±0.7	1.6	0.93	<0.001
	Mabounie	5.22±1.2	-27.1±3	1.9	0.79	<0.01
	Lopé h_1	3.91±1.07	-23.2±2.5	2.6	0.69	<0.05
	Lopé h_2	4.71±1.45	-25.1±3.5	2.1	0.68	<0.05
	Lopé h_3	6.24±1.76	-29.8±4.2	1.6	0.68	<0.05
	Paracou	7.89±1.8	-33.3±4.7	1.3	0.47	<0.001
Boreal & temperate	Alaska	2.37±0.67	-18.5±1.4	4.2	0.46	<0.001
	Maine	4.07±0.28	-21.8±0.9	2.5	0.86	<0.001
	Remningstorp (09/03/2007) h_1	4.73±0.4	-20.7±0.8	2.1	0.71	<0.001
	Remningstorp (02/04/2007) h_1	4.44±0.38	-20.6±0.8	2.2	0.71	<0.001
	Remningstorp (02/05/2007) h_1	4.24±0.35	-20.7±0.7	2.4	0.73	<0.001
	Remningstorp (09/03/2007) h_2	5.26±0.47	-21.5±0.9	1.9	0.71	<0.001
	Remningstorp (31/03/2007) h_2	4.25±0.43	-20±0.9	2.4	0.65	<0.001
	Remningstorp (02/05/2007) h_2	4.58±0.51	-20.8±1	2.2	0.63	<0.001
	Krycklan h_1	1.32±0.52	-16.2±1	7.6	0.21	<0.05
	Krycklan h_2	1.84±0.65	-17.8±1.3	5.4	0.25	<0.01
	Landes	10.14±0.84	-34.2±1.7	1.0	0.88	<0.001
	Tropical	5.18±0.29	-26.4±0.7	1.9	0.8	<0.001
	Boreal	4.64±0.22	-21.4±0.5	2.2	0.5	<0.001

The log-log fit between AGB and HV backscatter exhibits coefficients of determination (R^2) better than 0.46 except for the two Krycklan acquisitions (Tab. II), for which the R^2 values are 0.21 and 0.25. However, Krycklan has the smallest range of AGB values and strongest topography of all sites, and topography in particular has marked effects on the γ^0_{HV}-AGB relation [15]. The R^2 value was 0.8 for pooled tropical forest data and 0.5 for pooled boreal/temperate forest (Tab. II).

The slope parameter a of (1) is in most cases higher for the tropical sites than for boreal/temperate areas, but its highest value is for the plantation forest of Landes, France. Consequently, the exponent p in (2) is lower in the tropics than for boreal/temperate sites (Tab. II). The difference of the slopes between tropical, boreal and plantation forests is also reflected in the cross-comparison of the sites.

The slopes in tropical forest do not differ significantly (Tab. III), except between La Selva and Lopé h_1. There are no significant differences between the slopes for Mabounie, the three Lopé headings, Paracou, Maine and the various Remningstorp acquisitions nor, as expected, between the slopes for the Remningstorp acquisitions. In contrast, the slopes for Krycklan (which has hilly terrain [15]) and Landes (plantation forest) are significantly different from those at the other sites, as is the slope for Alaska (which has flat to moderate topography [12]) and most of the other sites. Differences between the slopes for the individual boreal/temperate sites and the pooled tropical data were in most cases insignificant, whereas most boreal/temperate sites have significantly different slopes than

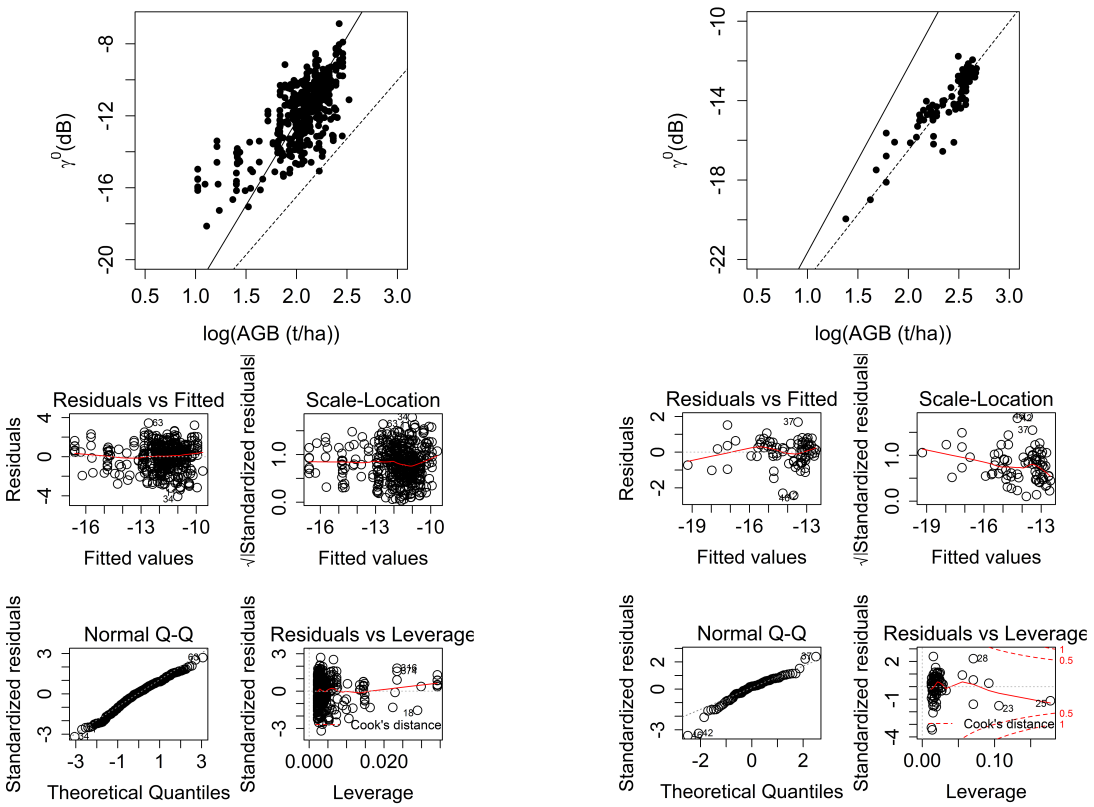

(a) Boreal/temperate (b) Tropical

Fig. 1. Scatterplots of HV backscatter (γ^0 [dB]) against aboveground biomass (t/ha) in (a) boreal/temperate and (b) tropical forest; both scatterplots also show the regression lines for the boreal (solid) and tropical data (dashed). Below each scatterplot is the associated plot of residuals versus fitted values, the quantile-quantile (Q-Q) plot, the scale-location plot, and the plot of residuals versus leverage.

the pooled tropical data.

As mentioned in Section III-B, the intercepts were only compared where slopes did not differ significantly. For these cases, the intercepts did not differ significantly between any of the pairs of individual sites except for Lopé h_3 and the boreal sites (Tab. IV). This is expected since the intercepts do not differ substantially between the different sites within each biome (Tab. II). However, the intercept of the pooled tropical data differs from those of the individual boreal sites and the pooled boreal/temperate data (Tab. IV).

V. Implications of the Power Law Relationship for BIOMASS Mission Performance

Although it is easier to estimate fitting parameters and investigate the quality of the model-data fits using the log-log relationship (1), the implications for BIOMASS performance and processing requirements are most easily analyzed using the power law relationship (2), so this is used throughout Section V.

A. Required effective number of looks

The power law model (2) provides a simple framework to estimate the ENL needed to meet the requirement for BIOMASS of a 20% error in AGB at 200 m resolution [11]. Differentiating (2) with respect to γ^0 gives

$$\frac{d\text{AGB}}{d\gamma^0} = 10^{-b/a} p (\gamma^0)^{p-1} \tag{9}$$

Approximating the derivative by the ratio of differences, we can therefore write the relative error in AGB associated with a relative error in γ^0, under the assumption that the error is not too large, as

$$\frac{\Delta\text{AGB}}{\text{AGB}} = p \frac{\Delta\gamma^0}{\gamma^0} \tag{10}$$

where Δ denotes difference. The 20% error requirement on AGB can thus be expressed as

$$\frac{\Delta\text{AGB}}{\text{AGB}} = p \frac{\Delta\gamma^0}{\gamma^0} < 0.2 \tag{11}$$

A variety of system error sources, including instrument noise, radiometric bias and accuracy, ambiguities, etc., contribute to the error in γ^0, but a significant component is due to speckle. If other error sources take up $0.2 - x$ of the relative error budget then the relative error in AGB due to speckle cannot exceed x (clearly x must be less than 0.2 if the requirement is ever to be met, and its true value will be better quantified when we have fuller knowledge about the

TABLE III
SIGNIFICANCE VALUES FOR THE HYPOTHESIS THAT SLOPES ARE DIFFERENT BETWEEN PAIRWISE COMBINATIONS OF SITES (GRAY TONES INDICATE A SIGNIFICANT DIFFERENCE WITH VERY LIGHT GRAY FOR 90%, LIGHT GRAY FOR 95%, GRAY 99% AND DARK GRAY FOR 99.9%, N.S. INDICATES THAT SLOPES ARE NOT SIGNIFICANTLY DIFFERENT).

Site	Mab.	Lopé h_1	Lopé h_2	Lopé h_3	Paracou	Alaska	Maine	Rem. t_1h_1	Rem. t_2h_1	Rem. t_3h_1	Rem. t_1h_2	Rem. t_2h_2	Rem. t_3h_1	Kryck. h_1	Kryck. h_2	Landes	Boreal	Tropical
La Selva	*n.s.*	<0.05	*n.s.*	*n.s.*	*n.s.*	<0.001	<0.05	<0.1	<0.05	<0.01	*n.s.*	<0.05	<0.01	<0.001	<0.001	<0.001	*n.s.*	*n.s.*
Mabounie		*n.s.*	*n.s.*	*n.s.*	*n.s.*	*n.s.*	*n.s.*	*n.s.*	*n.s.*	*n.s.*	*n.s.*	*n.s.*	*n.s.*	<0.05	*n.s.*	<0.05	*n.s.*	*n.s.*
Lopé h_1			*n.s.*	*n.s.*	*n.s.*	*n.s.*	*n.s.*	*n.s.*	*n.s.*	*n.s.*	*n.s.*	*n.s.*	*n.s.*	<0.05	<0.1	<0.001	*n.s.*	*n.s.*
Lopé h_2				*n.s.*	*n.s.*	*n.s.*	*n.s.*	*n.s.*	*n.s.*	*n.s.*	*n.s.*	*n.s.*	*n.s.*	<0.01	<0.05	<0.01	*n.s.*	*n.s.*
Lopé h_3					*n.s.*	<0.05	*n.s.*	*n.s.*	*n.s.*	<0.1	*n.s.*	*n.s.*	*n.s.*	<0.001	<0.01	<0.05	*n.s.*	*n.s.*
Paracou						<0.1	*n.s.*	*n.s.*	*n.s.*	*n.s.*	*n.s.*	*n.s.*	*n.s.*	<0.01	<0.05	*n.s.*	*n.s.*	*n.s.*
Alaska							<0.05	<0.01	<0.01	<0.01	<0.001	<0.05	<0.05	*n.s.*	*n.s.*	<0.001	<0.05	<0.001
Maine								*n.s.*	*n.s.*	*n.s.*	<0.1	*n.s.*	*n.s.*	<0.01	<0.05	<0.001	*n.s.*	<0.05
Rem. t_1h_1									*n.s.*	*n.s.*	*n.s.*	*n.s.*	*n.s.*	<0.001	<0.01	<0.001	*n.s.*	*n.s.*
Rem. t_2h_1										*n.s.*	*n.s.*	*n.s.*	*n.s.*	<0.001	<0.01	<0.001	*n.s.*	*n.s.*
Rem. t_3h_1											<0.1	*n.s.*	*n.s.*	<0.001	<0.01	<0.001	*n.s.*	<0.05
Rem. t_1h_2												*n.s.*	*n.s.*	<0.001	<0.001	<0.001	*n.s.*	*n.s.*
Rem. t_2h_2													*n.s.*	<0.001	<0.01	<0.001	*n.s.*	<0.1
Rem. t_3h_2														<0.001	<0.01	<0.001	*n.s.*	*n.s.*
Kryck. h_1															*n.s.*	<0.001	<0.01	<0.001
Kryck. h_2																<0.001	<0.05	<0.001
Landes																	<0.001	<0.001
Boreal																		*n.s.*

TABLE IV
SIGNIFICANCE VALUES FOR THE HYPOTHESIS THAT INTERCEPTS ARE DIFFERENT BETWEEN PAIRWISE COMBINATIONS OF SITES (GRAY TONES INDICATE A SIGNIFICANT DIFFERENCE WITH VERY LIGHT GRAY FOR 90%, LIGHT GRAY FOR 95%, GRAY 99% AND DARK GRAY FOR 99.9%, N.S. INDICATES THAT INTERCEPTS ARE NOT SIGNIFICANTLY DIFFERENT, COMBINATIONS WITH - HAVE A SIGNIFICANTLY DIFFERENT SLOPE).

Site	Mab.	Lopé h_1	Lopé h_2	Lopé h_3	Paracou	Alaska	Maine	Rem. t_1h_1	Rem. t_2h_1	Rem. t_3h_1	Rem. t_1h_2	Rem. t_2h_2	Rem. t_3h_1	Kryck. h_1	Kryck. h_2	Landes	Boreal	Tropical
La Selva	*n.s.*	-	*n.s.*	*n.s.*	*n.s.*	-	-	-	-	-	<0.001	-	-	-	-	-	<0.01	*n.s.*
Mabounie		*n.s.*	*n.s.*	*n.s.*	*n.s.*	*n.s.*	*n.s.*	*n.s.*	*n.s.*	*n.s.*	*n.s.*	*n.s.*	*n.s.*	-	<0.1	-	*n.s.*	*n.s.*
Lopé h_1			*n.s.*	*n.s.*	*n.s.*	*n.s.*	*n.s.*	*n.s.*	*n.s.*	*n.s.*	*n.s.*	*n.s.*	*n.s.*	-	-	-	*n.s.*	*n.s.*
Lopé h_2				*n.s.*	*n.s.*	*n.s.*	*n.s.*	*n.s.*	*n.s.*	<0.1	*n.s.*	*n.s.*	*n.s.*	-	-	-	*n.s.*	*n.s.*
Lopé h_3					*n.s.*	-	<0.05	<0.01	<0.01	-	<0.05	<0.01	<0.05	-	-	-	<0.1	*n.s.*
Paracou						-	*n.s.*	*n.s.*	*n.s.*	<0.1	*n.s.*	*n.s.*	*n.s.*	-	-	*n.s.*	*n.s.*	*n.s.*
Alaska							-	-	-	-	-	-	-	*n.s.*	*n.s.*	-	-	-
Maine								*n.s.*	*n.s.*	*n.s.*	-	*n.s.*	*n.s.*	-	-	-	*n.s.*	-
Rem. t_1h_1									*n.s.*	*n.s.*	*n.s.*	*n.s.*	*n.s.*	-	-	-	*n.s.*	<0.001
Rem. t_2h_1										*n.s.*	*n.s.*	*n.s.*	*n.s.*	-	-	-	*n.s.*	<0.001
Rem. t_3h_1											-	*n.s.*	*n.s.*	-	-	-	*n.s.*	-
Rem. t_1h_2												*n.s.*	*n.s.*	-	-	-	*n.s.*	<0.001
Rem. t_2h_2													*n.s.*	-	-	-	*n.s.*	-
Rem. t_3h_2														-	-	-	*n.s.*	<0.001
Kryck. h_1															*n.s.*	-	-	-
Kryck. h_2																-	-	-
Landes																	-	-
Boreal																		<0.001

BIOMASS system). Equating the absolute error in γ^0 due to speckle to the standard deviation associated with the ENL, L, then $\Delta\gamma^0_{Speckle} = \frac{\gamma^0}{\sqrt{L}}$. We therefore require

$$p\frac{\Delta\gamma^0_{Speckle}}{\gamma^0} = \frac{p}{\sqrt{L}} < x \tag{12}$$

Consequently, keeping the relative error due to speckle within the required bounds depends on the number of looks, L, and the exponent, p, in (2). Earlier end-to-end performance studies, based on Monte Carlo simulations under a simplified inversion scheme, suggest that about 10% (or half of the error budget) has to be allocated for system errors [11], so $x = 0.1$, and we then require

$$L > 100p^2. \tag{13}$$

Using (13) with the p values from the pooled boreal and pooled tropical data (Tab. II) indicates that the ENL required is 464 (boreal) and 373 (tropical). The lower values for the tropics arise from the lower exponent in (2). The required ENL for various values of the relative AGB error (i.e., the value of x in (12)) were further calculated using the p values from the pooled data (Fig. 2). (Note that in Fig. 2 the relative error is allowed to take values up to 30% even though the target maximum error for BIOMASS is 20%). Reducing the speckle-related relative error in AGB to 5% would require more than 1000 looks in all biomes.

Providing such a large number of looks while meeting the 200 m spatial resolution requirement is not possible for single BIOMASS images, since the allowable bandwidth of the BIOMASS system is restricted by International Telecommunication Union regulations to 6 MHz [11], which corresponds roughly to 50 m ground range resolution. Since the system is designed to give 6 looks in azimuth at 50 m resolution, spatial averaging will yield only 96 looks at 200 m resolution for a single image product. However, the accuracy requirements can be met by multi-channel filtering. This type of linear filter can exploit multi-temporal or multi-polarized acquisitions, or both. It causes minimal loss of spatial resolution, unlike spatial filtering and multi-looking techniques, while significantly increasing the ENL [31], [32].

A general expression for this filter is given in [32], where it is shown that for an input dataset of M registered intensity images, the output will be M intensity images which are

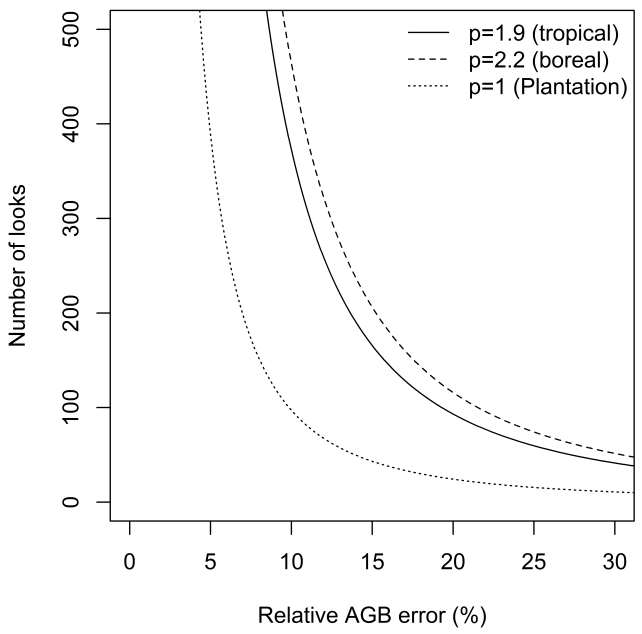

Fig. 2. Dependence of required number of looks on percentage relative error in aboveground biomass due to speckle for different power law exponents. In the figure the relative error (the term x in (12)) is allowed to take values up to 30% even though the target maximum error for BIOMASS is 20%.

unbiased (i.e. the radiometry is preserved in each image), have optimal speckle reduction, and which all have the same (local) ENL. In the simplest case of M uncorrelated input images with the same ENL, L, the filter has the form

$$J_k(x,y) = \frac{\hat{\sigma}_k(x,y)}{M}\sum_{i=1}^{M}\frac{I_i(x,y)}{\hat{\sigma}_i(x,y)}, 1 \le k \le M \tag{14}$$

where I_i and J_i, $i = 1, ..., M$, are the input and output images, respectively, (x, y) denotes position, and $\hat{\sigma}_i(x, y)$ denotes the local mean intensity at position (x, y) in input image i [32], [33]. A variety of spatial filters can be used to estimate the local mean intensity, but if we simply average over a window containing N independent pixels, the theoretical ENL in each output image will be approximately constant across the image and will have the value [32]

$$\text{ENL} = \frac{MNL}{M+N-1}. \tag{15}$$

This increases as the number of images increases, but the increase diminishes as each extra channel is added, fundamentally because the local mean intensity is estimated from the data, i.e, $\hat{\sigma}_i(x, y)$ is not known exactly.

In practice, however, some of the channels used for filtering may be correlated (e.g. the HH and VV polarizations from the same acquisition), in which case the ideal ENL is given by [32]

$$\text{ENL} = L\sum_{i,j=1}^{M} R_{ij}^{-1} \tag{16}$$

where $R_{ij}(x, y)$ is the local intensity correlation matrix. There is no known equivalent to (15) that takes into account the effect of estimating the local correlation matrix from the data, although we expect a similar slowdown in the increase of ENL as extra channels are added. However, if we assume that the co-polarized and cross-polarized channels are uncorrelated, while the local HH-VV intensity correlation coefficient is ρ, then it is easy to see from (16) that for a single polarimetric (HH, HV, VV) triplet

$$\text{ENL} = L\frac{3+\rho}{1+\rho} \tag{17}$$

For $L = 96$ this gives ENLs of 224 when $\rho = 0.5$ and 203 when $\rho = 0.8$. Subject to the slowdown in ENL gain indicated by (15), these values would be approximately doubled if we use ascending and descending images (which will be uncorrelated), assuming the local intensity correlation coefficients are the same in both images. Hence multi-channel filtering using ascending and descending images will be necessary to meet BIOMASS performance requirements in the tropics, but multi-temporal images will also be needed in the boreal zone. These will need to come from different orbit cycles because the orbit pattern for BIOMASS is designed to ensure high correlation between repeat images in the Tomographic and Interferometric phases [11]; hence their use in the filtering would provide only a small gain in ENL.

B. Estimating biomass change under a power law relation

Under a power law relation between AGB and γ^0, there is a simple relation between the relative change in AGB and a dB change in γ^0. For a change in γ^0 by x dB, we can write

$$10\log_{10}(\gamma^0 + \Delta\gamma^0) - 10\log_{10}\gamma^0 = 10\log_{10}(1 + \frac{\Delta\gamma^0}{\gamma^0}) = x \tag{18}$$

which is equivalent to

$$\frac{\Delta\gamma^0}{\gamma^0} = 10^{\frac{x}{10}} - 1. \tag{19}$$

Using (10), under small changes in AGB the associated relative biomass change is

$$\frac{\Delta\text{AGB}}{\text{AGB}} = p\frac{\Delta\gamma^0}{\gamma^0} = p(10^{\frac{x}{10}} - 1) \tag{20}$$

Hence the relative change in AGB associated with a given dB change is independent of the AGB or γ^0 value and depends only on the HV backscatter change x and the exponent p of the power law (2).

Another way to interpret (10) is in terms of the error in estimated relative biomass change when there are changes in the signal caused by uncorrected environmental changes (e.g. changes in vegetation water content, soil moisture, freeze/thaw, etc.) or variation in the system radiometry. As for the ENL, the impact of such errors is generally smaller in tropical forest than boreal forest due to the smaller exponent p. A residual error of 1 dB will cause a relative biomass change error of 56% (boreal) and 50% (tropical) (Fig. 3). To achieve a

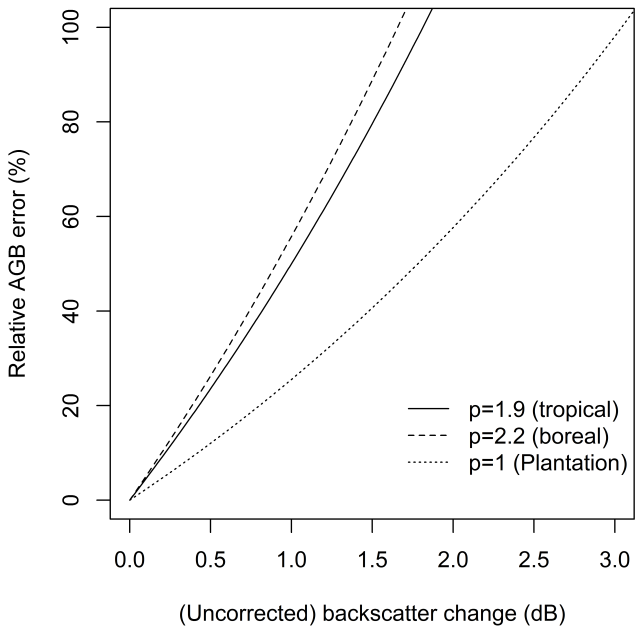

Fig. 3. Relation between backscatter change in dB and relative error/change in aboveground biomass for different power law exponents.

relative accuracy of 20% or better, residual signals (including uncorrected environmental signals, instrument effects, etc.) should not exceed 0.43 dB for tropical and 0.39 dB for boreal forests (Fig. 3).

C. Logarithmic bias

The fitting of a linear model in log-log space assumes an additive zero-mean random error term ϵ in the observations. However, after transformation to natural units the power law model contains a multiplicative error term which can result in a bias [34]–[37]:

$$\text{AGB} = 10^{-b/a}(\gamma^0_{HV})^p 10^{\epsilon}. \tag{21}$$

This bias can be corrected if we estimate the value of 10^{ϵ} by calculating the mean squared error (MSE) of the regression as

$$\text{MSE} = \frac{\sum_{i=1}^{n} e_i^2}{n-2} \tag{22}$$

where e is the regression residual of the ith data pair and n is the number of pairs [34]. We can then set $10^{\epsilon} = 10^{MSE/2}$ [34], [37] if the data are normally distributed, otherwise we should use the expression [34], [36]

$$10^{\epsilon} = \frac{\sum_{i=1}^{n} 10^{e_i}}{n}. \tag{23}$$

VI. Discussion

Radar backscatter is not a direct measurement of AGB [21], but is a function of forest structure and dielectric and consequently is correlated with AGB. Numerous earlier studies exploited a logarithmic model to describe the relationship between HV backscatter and AGB [8]–[10], [12]–[19], [38], but most of these studies were limited to one or two areas in a single biome and did not assess the general applicability of such a model. In this study, a systematic analysis confirms that to first order a logarithmic model can be used to describe the relationship between HV backscatter and AGB across nine sites in boreal, hemi-boreal, temperate and tropical forest, as well as a managed temperate plantation forest. This observed consistency of the linear logarithmic model is remarkable, given the range of forest types and conditions in our dataset, and the fact that, for airborne systems, the incidence angle can range from 25° to 55°, and hence the dominant scattering mechanisms may differ substantially across the swath. The estimated slopes, intercepts and coefficients of determination were generally in good agreement with values reported in the literature (e.g [9], [13]), except where topography was a major perturbing factor (e.g. at Krycklan [15]).

Despite the empirical support for the logarithmic model, currently little is known about what determines the slope of this relationship (although the intercept is in principle determined by the soil scattering if the power law holds down to small values of biomass). However, physical models have been developed in order to simulate the SAR backscatter as a function of biomass [39]–[41]. One example is the Multi-static Interferometric Polarimetric Electromagnetic model for Remote Sensing (MIPERS), in which the vegetation scatterers are modeled as canonical elements, i.e., dielectric cylinders for branches or trunks and ellipsoids for leaves [20], [40], [41]. The relationship between AGB and γ^0 given by MIPERS was found to be adequately described by a logarithmic model [20], but this did not lead to any simple description of how the associated power law exponent p was related to the model parameters.

Cross-comparison using Analysis of Covariance indicated that similar logarithmic models were valid across most study areas, especially when similar ranges of biomass were compared. This agrees with analysis in [9] which indicated similar logarithmic relationships between HV backscatter and biomass for coniferous and evergreen broad-leaf forest. The model coefficients for high biomass tropical forests and low biomass boreal forests were significantly different, which concurs with [13], in which significantly different slopes and R^2 values were reported for low and high biomass forests. As a consequence, the regression for the pooled boreal/temperate data, which cover a large range of biomass, is not significantly different from those for the individual tropical sites. In contrast, the tropical data have fewer low biomass values and so the regression lines for pooled tropical data and the individual boreal/temperate sites differ significantly in all cases (either the slopes are significantly different or, if not, the intercepts are (Tab. III and IV)). Substantial differences were also observed between the boreal forest of Krycklan and the hemi-boreal forest of Remningstorp [15], but this comparison is confused by the fact that Krycklan is a much hillier site, as well as having a different range of biomass. Note that, in contrast, the study in [15] found similar logarithmic regression coefficients for these two sites and that the slope for Krycklan was much larger than in Tab. II. The values given for a in [15] (after rearranging the relevant equation) are 7.143 for Remningstorp

and 6.711 for Krycklan, with associated power law exponents p = 1.40 and 1.49, respectively. This could be because [15] used AGB estimates supported by laser scanning for 97 plots in Krycklan with different areal coverage and range of AGB than the 27 stands used in this study. In Krycklan, higher AGB is generally found on steeper terrain. The AGB of the stands we used is non-uniformly distributed on slopes and has a different distribution of AGB on slopes than in [15]. This results in different sensitivity of γ^0 to AGB and consequently a different power law exponent in the two datasets. The regression in the Landes forest was significantly different from all other forest types; although the Landes site is very dissimilar to the other sites, being a plantation forest with very homogeneous monocultural stands on flat topography [8], the physical reasons underlying such different behaviour are not known. In general, further study of what determines the power law exponent is needed, because Section V makes clear this exponent has important effects on the ENL needed to recover AGB to a given relative accuracy.

It might be expected that differences in the intercepts could be explained by different site and environmental conditions, assuming that the power law is appropriate down to low biomass values. However, the only site at which soil moisture was measured was Remningstorp, and here the results suggest that soil moisture has only a small effect on the AGB-γ_0 relationship, since acquisitions under different moisture conditions resulted in similar models, as previously noted in [14]. This indicates a need for further study of how environmental conditions affect P-band returns for very low biomass. However, it should be noted that there may be calibration errors in the different instruments providing the datasets analyzed in this study, which would give absolute backscatter biases between them but would not alter the slopes of the regressions.

Although the analysis reported here is based on airborne data, simulations of BIOMASS performance indicate that a similar relation between backscatter and AGB would be expected [11], [42], [43]. In addition, spaceborne SAR systems need to account for ionospheric effects (especially Faraday rotation) and possible calibration errors. Assuming that $S_{HV} = S_{VH}$ (where S_{HV} and S_{VH} are respectively the HV and VH complex backscattering coefficients), it is shown in [44] that without calibration errors the maximum likelihood estimate of S_{HV} (and hence γ^0_{HV}) is unaffected by Faraday rotation. When calibration errors are also present there is a complex interaction with Faraday rotation, leading to errors in γ^0_{HV}. The ensuing errors in the estimated biomass under a power law model are analyzed in detail in [44], together with conditions on channel imbalance and cross-talk if the relative error in biomass is to not exceed a specified value (20% being the target for the BIOMASS mission [10], [11]).

It should be noted that the HH/VV polarization ratio and slope information have been used to reduce topographic effects in Krycklan [15], and topographic correction using the polarization orientation angle was applied for Paracou in [19]. Here we applied only a simple first order topographic correction to the data ($\gamma^0_{HV} = \sigma^0_{HV}/\cos\theta$) in order to have comparable backscattering coefficients for all sites. It is likely that some of the differences in regression coefficients for regions with similar forest types are caused by residual topographic effects, especially for sites such as Lopé with substantial topographic variation. Further topographic correction using channels other than HV will almost certainly be needed in a more complete algorithm for recovering AGB from polarimetric data, and this can be expected to modify the regression coefficients.

VII. Conclusions

The analysis in this paper is relevant for any SAR sensor estimating biomass from measurements on the basis of a power law, but its greatest significance is at P-band where our extensive empirical analysis confirms the generality of the relationship between HV backscatter and AGB across a wide range of airborne datasets [8]–[19]. However, a power law was also frequently found to be appropriate at other wavelengths [9], [13], [16], [18], [20] and from modeling [20]. The regressions for tropical and boreal data were found to be significantly different which implies that the regression model needs to be adjusted to the forest type. Under a power law relationship, it was shown that accurate estimates of biomass require an ENL whose value depends crucially on the exponent of the power law, with smaller exponents giving better relative accuracies. The smallest exponent was found in plantation forest, and tropical forest exhibited a smaller exponent than boreal forest. This implies that boreal forests will need a higher ENL than tropical forests in order to meet BIOMASS requirements. A very important conclusion in terms of BIOMASS data processing is that both boreal and tropical forest will require an ENL whose value exceeds that available in a single polarimetric image BIOMASS product (i.e., an ENL of around 96). This implies that multi-channel filtering [11], [32], [43] will be needed in order to increase the ENL without degrading the spatial resolution. In the filtering, combining the HV channel with a co-polarized channel will roughly double the ENL because of the low correlation between these channels, but adding the second co-polarized channel gives less gain in ENL because of the correlation between the HH and VV channels [43]. Using repeat images from the Interferometric or Tomographic Phases of the mission as inputs to the filtering will bring little gain in ENL since, by design, there will be strong correlation between them [43], [45]. Therefore, it will be necessary to combine data from ascending and descending passes (which will be uncorrelated) and/or from different orbit cycles (for which we would expect little or no correlation in forested areas).

Furthermore, the relative change in AGB associated with a relative change in γ^0_{HV} is, to first order, proportional to the exponent and independent of the absolute biomass value. This places stringent conditions on the acceptable level of uncorrected disturbance to the HV backscatter from environmental (e.g. moisture, topography and freeze/thaw) and system effects if BIOMASS is to meet its performance requirements. Any residual error will result in an AGB estimation error, and to achieve the required AGB accuracy of 20% for BIOMASS mission, the residual backscatter error should not exceed 0.39 dB in the worst case of boreal forest. The same analysis is

also important for measuring biomass disturbance: the biomass change must exceed 20% in order to be detected if the backscatter correction is to an accuracy of 0.39 dB.

Our findings are based purely on the γ^0_{HV}-AGB relationship, while extra information about biomass may be obtained by use of more polarizations and information derived from Polarimetric SAR interferometry and SAR tomography [10], [11], [22], [46]. However, similar constraints on ENL and change are likely for these more advanced methods since they rely on AGB-backscatter relations that are approximately power laws, especially in the higher ranges of biomass.

ACKNOWLEDGMENT

The authors would like to thank all campaign teams and in particular Thuy Le Toan for preparing and providing the data from Paracou, Landes, Maine, La Selva and Alaska, and Lars Ulander for preparing and providing the data from Remningstorp.

REFERENCES

[1] GCOS, *Status of the Global Observing System for Climate*. WMO, 2015, GCOS-195.

[2] Y. Pan, R. A. Birdsey, J. Fang, R. Houghton, P. E. Kauppi, W. A. Kurz, O. L. Phillips, A. Shvidenko, S. L. Lewis, J. G. Canadell, P. Ciais, R. B. Jackson, S. W. Pacala, A. D. McGuire, S. Piao, A. Rautiainen, S. Sitch, and D. Hayes, "A large and persistent carbon sink in the world's forests," *Science*, vol. 333, no. 6045, pp. 988–993, 2011. [Online]. Available: http://science.sciencemag.org/content/333/6045/988

[3] Y. Y. Liu, A. I. J. M. van Dijk, R. A. M. de Jeu, J. G. Canadell, M. F. McCabe, J. P. Evans, and G. Wang, "Recent reversal in loss of global terrestrial biomass," *Nature Climate Change*, vol. 5, p. 470474, 2015.

[4] M. A. Lefsky, D. J. Harding, M. Keller, W. B. Cohen, C. C. Carabajal, F. Del Bom Espirito-Santo, M. O. Hunter, and R. de Oliveira, "Estimates of forest canopy height and aboveground biomass using icesat," *Geophysical Research Letters*, vol. 32, no. 22, pp. 1–4, 2005.

[5] T. Hu, Y. Su, B. Xue, J. Liu, X. Zhao, J. Fang, and Q. Guo, "Mapping global forest aboveground biomass with spaceborne lidar, optical imagery, and forest inventory data," *Remote Sensing*, vol. 8, no. 7, pp. 565–591, 2016.

[6] A. Baccini, S. J. Goetz, W. S. Walker, N. T. Laporte, M. Sun, D. Sulla-Menashe, J. Hackler, P. S. A. Beck, R. Dubayah, M. A. Friedl, S. Samanta, and R. A. Houghton, "Estimated carbon dioxide emissions from tropical deforestation improved by carbon-density maps," *Nature Climate Change*, vol. 2, 2012.

[7] S. S. Saatchi, N. L. Harris, S. Brown, M. Lefsky, E. T. A. Mitchard, W. Salas, B. R. Zutta, W. Buermann, S. L. Lewis, S. Hagen, S. Petrova, L. White, M. Silman, and A. Morel, "Benchmark map of forest carbon stocks in tropical regions across three continents," *Proceedings of the National Academy of Science of the United States of America (PNAS)*, vol. 108, no. 24, pp. 9899–9904, 2011a.

[8] T. Le Toan, A. Beaudoin, J. Riom, and D. Guyon, "Relating forest biomass to sar data," *IEEE Transactions on Geoscience and Remote Sensing*, vol. 30, no. 2, pp. 403–411, 3 1992.

[9] M. L. Imhoff, "Radar backscatter and biomass saturation: ramifications for global biomass inventory," *IEEE Transactions on Geoscience and Remote Sensing*, vol. 33, no. 2, pp. 511–518, Mar 1995.

[10] T. Le Toan, S. Quegan, M. Davidson, H. Balzter, P. Paillou, K. Papathanassiou, S. Plummer, F. Rocca, S. Saatchi, H. Shugart, and L. Ulander, "The biomass mission: Mapping global forest biomass to better understand the terrestrial carbon cycle," *Remote Sensing of Environment*, vol. 115, no. 11, pp. 2850–2860, 2011, {DESDynI} VEG-3D Special Issue.

[11] ESA, *Report for Mission Selection: Biomass, ESA SP-1324/1*. Noordwijk: European Space Agency, 2012.

[12] E. Rignot, J. Way, C. Williams, and L. Viereck, "Radar estimates of aboveground biomass in boreal forests of interior alaska," *IEEE Transactions on Geoscience and Remote Sensing*, vol. 32, no. 5, pp. 1117–1124, Sep 1994.

[13] K. J. Ranson and G. Sun, "Mapping biomass of a northern forest using multifrequency sar data," *IEEE Transactions on Geoscience and Remote Sensing*, vol. 32, no. 2, pp. 388–396, Mar 1994.

[14] G. Sandberg, L. Ulander, J. Fransson, J. Holmgren, and T. L. Toan, "L- and p-band backscatter intensity for biomass retrieval in hemiboreal forest," *Remote Sensing of Environment*, vol. 115, no. 11, pp. 2874 – 2886, 2011, dESDynI VEG-3D Special Issue. [Online]. Available: http://www.sciencedirect.com/science/article/pii/S0034425711001350

[15] M. J. Soja, G. Sandberg, and L. M. H. Ulander, "Regression-based retrieval of boreal forest biomass in sloping terrain using p-band sar backscatter intensity data," *IEEE Transactions on Geoscience and Remote Sensing*, vol. 51, no. 5, pp. 2646–2665, May 2013.

[16] D. H. Hoekman and M. J. Quinones, "Land cover type and biomass classification using airsar data for evaluation of monitoring scenarios in the colombian amazon," *IEEE Transactions on Geoscience and Remote Sensing*, vol. 38, no. 2, pp. 685–696, Mar 2000.

[17] T. Neeff, L. V. Dutra, J. R. dos Santos, C. d. C. Freitas, and L. S. Araujo, "Tropical forest measurement by interferometric height modeling and p-band radar backscatter," *Forest Science*, vol. 51, no. 6, pp. 585–594, 2005. [Online]. Available: http://www.ingentaconnect.com/content/saf/fs/2005/00000051/00000006/art00009

[18] S. Saatchi, M. Marlier, R. L. Chazdon, D. B. Clark, and A. E. Russell, "Impact of spatial variability of tropical forest structure on radar estimation of aboveground biomass," *Remote Sensing of Environment*, vol. 115, no. 11, pp. 2836–2849, 2011. [Online]. Available: http://www.sciencedirect.com/science/article/pii/S0034425711001313

[19] L. Villard and T. Le Toan, "Relating p-band sar intensity to biomass for tropical dense forests in hilly terrain: γ^0 or t^0?" *IEEE Journal of Selected Topics in Applied Earth Observations and Remote Sensing*, vol. 8, no. 1, pp. 214–223, Jan 2015.

[20] S. Mermoz, M. Rejou-Mechain, L. Villard, T. L. Toan, V. Rossi, and S. Gourlet-Fleury, "Decrease of l-band sar backscatter with biomass of dense forests," *Remote Sensing of Environment*, vol. 159, pp. 307 – 317, 2015. [Online]. Available: http://www.sciencedirect.com/science/article/pii/S0034425714005112

[21] I. H. Woodhouse, E. T. A. Mitchard, M. Brolly, D. Maniatis, and C. M. Ryan, "Radar backscatter is not a 'direct measure' of forest biomass," *Nature Climate Change*, vol. 2, pp. 556–557, 2012.

[22] M.-L. Truong-Loi, S. S. Saatchi, and S. Jaruwatanadilok, "Soil moisture estimation under tropical forests using uhf radar polarimetry," *IEEE Transactions on Geoscience and Remote Sensing*, vol. 53, no. 4, pp. 1718–1727, 2015.

[23] I. Hajnsek, M. Pardini, M. Jger, R. Horn, J. S. Kim, H. Jrg, K. Papathanassiou, P. Dubois-Fernandez, X. Dupuis, V. Wasik, S. Lewis, N. Labriere, L. Villard, and T. Koleck, *Technical Assistance for the Development of Airborne SAR and Geophysical Measurements During the AfriSAR Experiment*, T. Casal, Ed. ESA, 2017.

[24] P. Dubois-Fernandez, T. Le Toan, J. Chave, L. Blanc, S. Daniel, H. Oriot, A. Arnaubec, M. Rejou-Mechain, L. Villard, Y. Lasne, and T. Koleck, *TropiSAR 2009 - Technical Assistance for the Development of Airborne SAR and Geophysical Measurements during the TropiSAR 2009 Experiment*, M. Davidson and S. Cherchali, Eds. ESA/CNES, 2011, vol. 2.1.

[25] I. Hajnsek, R. Scheiber, L. Ulander, A. Gustavsson, G. Sandberg, S. Tebaldini, A. M. Guarnieri, F. Rocca, F. Bombardini, and M. Pardini, *BIOSAR 2007 - Technical Assistance for the Development of Airborne SAR and Geophysical Measurements during the BioSAR 2007 Experiment. Final Report*, M. Davidson, Ed. ESA, 2008, vol. 1.

[26] I. Hajnsek, R. Scheiber, M. Keller, R. Horn, S. Lee, L. Ulander, A. Gustavsson, G. Sandberg, T. Le Toan, S. Tebaldini, A. M. Guarnieri, and F. Rocca, *BIOSAR 2008 - Technical Assistance for the Development of Airborne SAR and Geophysical Measurements during the BioSAR 2008 Experiment. Final Report*, M. Davidson, Ed. ESA, 2009, vol. 1.

[27] M. Kutner, C. Nachtsheim, J. Neter, M. Li, W.Kutner, C. Nachtsheim, J. Neter, and W. Li, *Applied Linear Statistical Models*, 5th ed. New York: McGraw-Hill/Irwin, 2005.

[28] J. J. Faraway, *Extending the Linear Model with R. Generalized Linear, Mixed Effects and Nonparametric Regression Models*. Boca Raton: Chapman & Hall/CRC, 2006.

[29] J. M. Chambers, "Linear models," in *Statistical Models in S*, J. M. Chambers and T. J. Hastie, Eds. Pacific Grove: Wadsworth & Brooks/Cole Advanced Books & Software, 1992.

[30] G. A. F. Seber and A. J. Lee, *Linear regression analysis*. New Jersey: Wiley & Sons, 2003.

[31] J. Bruniquel and A. Lopes, "Multi-variate optimal speckle reduction in sar imagery," *International Journal of Remote Sensing*, vol. 18,

no. 3, pp. 603–627, 1997. [Online]. Available: http://dx.doi.org/10.1080/014311697218962

[32] S. Quegan and J. J. Yu, "Filtering of multichannel sar images," *IEEE Transactions on Geoscience and Remote Sensing*, vol. 39, no. 11, pp. 2373–2379, Nov 2001.

[33] S. Quegan, T. Le Toan, J. Yu, F. Ribbes, and N. Floury, "Multitemporal ers sar analysis applied to forest mapping," *IEEE Transactions on Geoscience and Remote Sensing*, vol. 38, no. 2, pp. 741 –753, mar 2000.

[34] M. Newman, "Regression analysis of log-transformed data: Statistical bias and its correction," *Environmental Toxicology and Chemistry*, vol. 12, pp. 1129–1133, 1993.

[35] G. L. Baskerville, "Use of logarithmic regression in the estimation of plant biomass," *Canadian Journal of Forest Research*, vol. 2, no. 1, pp. 49–53, 1972. [Online]. Available: https://doi.org/10.1139/x72-009

[36] N. Duan, "Smearing estimate: A nonparametric retransformation method," *Journal of the American Statistical Association*, vol. 78, no. 383, pp. 605–610, 1983. [Online]. Available: http://www.tandfonline.com/doi/abs/10.1080/01621459.1983.10478017

[37] J. Chave, C. Andalo, S. Brown, M. Cairns, J. Chambers, D. Eamus, H. Folster, F. Fromard, N. Higuchi, T. Kira *et al.*, "Tree allometry and improved estimation of carbon stocks and balance in tropical forests," *Oecologia*, vol. 145, no. 1, pp. 87–99, 2005.

[38] N. Baghdadi, G. L. Maire, J. S. Bailly, K. Os, Y. Nouvellon, M. Zribi, C. Lemos, and R. Hakamada, "Evaluation of alos/palsar l-band data for the estimation of eucalyptus plantations aboveground biomass in brazil," *IEEE Journal of Selected Topics in Applied Earth Observations and Remote Sensing*, vol. 8, no. 8, pp. 3802–3811, Aug 2015.

[39] F. T. Ulaby, K. Sarabandi, K. McDONALD, M. Whitt, and M. C. Dobson, "Michigan microwave canopy scattering model," *International Journal of Remote Sensing*, vol. 11, no. 7, pp. 1223–1253, 1990. [Online]. Available: http://dx.doi.org/10.1080/01431169008955090

[40] L. Villard, P. Borderies, T. L. Toan, T. Koleck, and C. Albinet, "Topography effects on forest radar scattering, consequences on biomass retrieval," in *IEEE International Geoscience and Remote Sensing Symposium 2010*, July 2010, pp. 60–63.

[41] L. Villard and P. Borderies, "Backscattering border eects for forests at c-band," *PIERS online*, vol. 3, no. 5, pp. 731–735, 2007.

[42] R. Scheiber, S. K. Lee, K. P. Papathanassiou, and N. Floury, "Extrapolation of airborne polarimetric and interferometric sar data for validation of bio-geo-retrieval algorithms for future spaceborne sar missions," in *IEEE International Geoscience and Remote Sensing Symposium 2009*, vol. 2, July 2009, pp. II–941–II–944.

[43] M. Schlund, K. Scipal, and M. W. Davidson, "Forest classification and impact of biomass resolution on forest area and aboveground biomass estimation," *International Journal of Applied Earth Observation and Geoinformation*, vol. 56, pp. 65 – 76, 2017. [Online]. Available: http://www.sciencedirect.com/science/article/pii/S0303243416302008

[44] S. Quegan and M. Lomas, "The interaction between faraday rotation and system effects in synthetic aperture radar measurements of backscatter and biomass," *IEEE Transactions on Geoscience and Remote Sensing*, vol. 53, no. 8, pp. 4299–4312, Aug. 2015.

[45] P. Dubois-Fernandez, T. L. Toan, S. Daniel, H. Oriot, J. Chave, L. Blanc, L. Villard, M. Davidson, and M. Petit, "The tropisar airborne campaign in french guiana: Objectives, description, and observed temporal behavior of the backscatter signal," *IEEE Transactions on Geoscience and Remote Sensing*, vol. 50, no. 8, pp. 3228–3241, 8 2012.

[46] D. H. T. Minh, T. L. Toan, F. Rocca, S. Tebaldini, M. M. d'Alessandro, and L. Villard, "Relating p-band synthetic aperture radar tomography to tropical forest biomass," *IEEE Transactions on Geoscience and Remote Sensing*, vol. 52, no. 2, pp. 967–979, Feb 2014.

Michael Schlund received the B.Sc. degree in geography, the M.Sc. degree in geoinformatics and remote sensing and Ph.D. degree from the Friedrich-Schiller-University Jena, Jena, Germany, in 2008, 2011 and 2015, respectively. In 2016, he joined the European Space Agency as Research Fellow in the Mission Science Division. Since 2018 he is with the Cartography, GIS and Remote Sensing Section of the University of Goettingen. His research focuses on forest monitoring and aboveground biomass retrieval algorithms based on polarimetric and interferometric synthetic aperture radar (SAR) data.

Klaus Scipal received the M.Sc. in Geodesy and the Ph.D. in remote sensing from the Vienna University of Technology (TUW), Austria, in 1999 and 2002 respectively. From 2002 to 2006 he was an Assistant Professor at the TUW leading the scatterometer group. In 2006 he joined the satellite data assimilation section of the European Centre for Medium Range Weather Forecasts, working on the land surface assimilation system. Since 2009 he is with the Mission Science Division of the European Space Agency contributing to the definition and development of earth observation satellites.

Shaun Quegan received his B.A. in mathematics and M.Sc. in mathematical statistics from the University of Warwick, then taught for seven years before undertaking a PhD in upper atmosphere/ionosphere modelling at the University of Sheffield. He joined Marconi Research Centre in 1982, becoming Remote Sensing Applications Group Chief in 1984. After joining the University of Sheffield in 1986, he built up a radar research group, and in 1993 helped to inaugurate and became Director of the Sheffield Centre for Earth Observation Science. In 2001 he became Director of the NERC Centre of Excellence in Terrestrial Carbon Dynamics and became leader of the Carbon Cycle Theme in the UK National Centre for Earth Observation (NCEO) when it was inaugurated in 2008. He was a lead proposer of the ESA BIOMASS mission and chairs the Mission Advisory Group. He is a member of the Terrestrial Observations Panel on Climate, the JAXA Kyoto and Carbon Panel (leading a project on monitoring deforestation in Indonesia & Brazil), was Chairman of the Terrestrial Carbon Observations Panel, and was a member of ESA???s Earth Science Advisory Committee from 2002-2007.